J Pharmacol Sci **120**, 26 – 35 (2012)

Journal of Pharmacological Sciences

Full Paper

Methylglyoxal Accumulation in Arterial Walls Causes Vascular Contractile Dysfunction in Spontaneously Hypertensive Rats

Masashi Mukohda[1], Muneyoshi Okada[1], Yukio Hara[1], and Hideyuki Yamawaki[1,*]

[1]*Laboratory of Veterinary Pharmacology, School of Veterinary Medicine, Kitasato University, Aomori 034-8628, Japan*

Received April 3, 2012; Accepted July 4, 2012

Abstract. Methylglyoxal (MGO) is a metabolite of glucose and perhaps mediates diabetes-related macrovascular complications including hypertension. In the present study, we examined if MGO accumulation affects vascular reactivity of isolated mesenteric artery from spontaneously hypertensive rats (SHR). Five-week-old SHR were treated with an MGO scavenger, aminoguanidine (AG), for 5 weeks. AG partially normalized increased blood pressure in SHR. In mesenteric artery from SHR treated with AG, increased accumulation of MGO-derived advanced glycation end-products was reversed. In mesenteric artery from SHR, AG normalized impaired acetylcholine (ACh)-induced relaxation and increased angiotensin (Ang) II-induced contraction. Reactive oxygen species (ROS) production increased in SHR mesenteric artery, and acute treatment with a nicotinamide adenine dinucleotide phosphate (NADPH) oxidase (NOX) inhibitor augmented ACh-induced relaxation. Protein expression of NOX1 and Ang II type 2 receptor (AT2R) increased in SHR mesenteric artery, which was normalized by AG. Acute treatment with an AT2R blocker but not a NOX inhibitor normalized the increased Ang II-induced contraction in SHR mesenteric artery. The present results demonstrate that MGO accumulation in mesenteric artery may mediate development of hypertension in SHR at least in part via increased ROS-mediated impairment of endothelium-dependent relaxation and AT2R-mediated increased Ang II contraction.

Keywords: glucose metabolite, smooth muscle, endothelium, vascular reactivity, reactive oxygen species

Introduction

Methylglyoxal (MGO) is a reactive dicarbonyl chemical that is produced in diverse biochemical processes. In the case of the non-enzymatic pathway, MGO is spontaneously formed in a process of glycolysis from dihydroxyacetone phosphate as a by-product of glyceraldehyde 3-phosphates in the cells including vascular endothelial cells (1) and smooth muscle cells (2). In addition, MGO is formed in some enzymatic processes by enzymes including cytochrome P450 (CYP) 2E1, MGO synthase, and semicarbazide-sensitive amine oxidase (SSAO) (3). Because MGO has two carbonyl groups, it can react with DNA, RNA, and protein (4). Specifically, MGO binds to and modifies lysine, arginine, and cysteine residues in proteins, which causes a non-enzymatic formation of several advanced glycation end-products (AGEs) (5) including N^{ε}-(carboxyethyl) lysine (CEL) (6), argpyrimidine (7), and the hydroimidazolone N^{ε}-(5-hydro-5-methyl-4-imidazolon-2-yl)-ornithine (8). MGO is degraded to D-lactic acid in the presence of glutathione by the glyoxalase system (4).

A recent report demonstrated that elevation of blood pressure (BP) of type 2 diabetic patients was associated with increase of plasma MGO level (9). Moreover, a previous report demonstrated that MGO accumulated in aorta of spontaneously hypertensive rats (SHR) with aging and that the increased MGO accumulation correlated with increase of BP (10). In addition, the increased MGO accumulation in the vasculature from women with preeclampsia was reported (11). It was also demonstrated that treatment with MGO given in drinking water not only increased BP in Wistar-Kyoto rats (WKY) (12) but also caused salt-sensitive hypertension and insulin resistance in Sprague–Dawley rats (13). These reports collectively indicate that MGO could directly affect vascular

*Corresponding author. yamawaki@vmas.kitasato-u.ac.jp
Published online in J-STAGE on August 23, 2012 (in advance)
doi: 10.1254/jphs.12088FP

reactivity of blood vessels. However, available reports were very limited. To overcome this, we have demonstrated by an in vitro study that short-term (30 min) treatment of endothelium-denuded rat aorta and mesenteric artery with MGO inhibited noradrenaline (NA)-induced contraction via activating smooth muscle large conductance Ca^{2+}-activated K^+ (BK_{Ca})-channel (14). Moreover, we have demonstrated that short-term treatment of rat aorta with MGO enhanced sodium nitroprusside (SNP)-induced endothelium-independent relaxation through activation of BK_{Ca}-channel, while short-term treatment of aorta with MGO had no effect on acetylcholine (ACh)-induced endothelium-dependent relaxation (15). We have also shown that short-term treatment of rat carotid artery with MGO augmented angiotensin (Ang) II-induced contraction via increasing endothelium-produced reactive oxygen species (ROS) (16). In addition, by using an organ-culture technique we have recently demonstrated that long-term (72 h) treatment of endothelium-denuded rat mesenteric artery with MGO inhibited NA-induced contraction, which is likely mediated via increased nicotinamide adenine dinucleotide phosphate (NADPH) oxidase (NOX) 1-derived superoxide production and subsequent apoptosis of smooth muscle (17). However, it remains to be clarified how the accumulated MGO is affecting vascular reactivity in vivo. Therefore in the present study, we sought to clarify the effects of MGO accumulation in vascular walls on vascular reactivity using SHR. Here, we demonstrated that MGO accumulation in mesenteric artery may mediate development of hypertension in SHR at least in part via increased Ang II-induced contraction and impairment of endothelium-dependent relaxation.

Materials and Methods

Chemicals

The chemicals used were as follows: ACh (Daiichi Pharmaceutical, Tokyo); aminoguanidine (AG) (Cayman, Ann Arbor, MI, USA); Ang II, NA, and SNP (Sigma-Aldrich, St. Louis, MO, USA); gp91ds-tat (Anaspec, Fremont, CA, USA); PD123319 (Wako, Osaka).

The antibody sources were as follows: Ang II type 2 receptor (AT2R) and NOX1 (GeneTex, Irvine, CA, USA); superoxide dismutase (SOD)-1 and SOD-2 (StressMarq Biosciences, Victoria, BC, Canada); SOD-3 (Assay Designs, Ann Arbor, MI, USA); endothelial nitric oxide (NO) synthase (eNOS) (Santa Cruz Biotech, Santa Cruz, CA, USA); $gp91^{phox}$ (NOX2) (BD Biosciences, Mississauga, ON, Canada); total actin (Sigma-Aldrich).

Animals

All animal care and treatment were conducted in conformity with the institutional guidelines of The Kitasato University and the National Institutes of Health Guide for the Care and Use of Laboratory Animals. WKY and SHR (Hoshino Laboratory Animals, Inc., Bando) were maintained on a standard laboratory diet and exposed to a 12 h / 12 h light-dark cycle at 23°C ± 2°C. Experiments were performed using 5 – 10-week-old rats. Rats were divided into 3 groups: WKY group, SHR group, and AG (1 g/L in drinking water for 5 weeks)-treated SHR group (SHR+AG).

BP measurements

Measurements of systolic BP (SBP), mean BP (MBP), and diastolic BP (DBP) in WKY, SHR, and SHR+AG were performed using a tail-cuff method (Softron, Tokyo) at a weekly interval from 5 to 10 weeks of age. Rats were trained before starting the measurement to reduce stress and were heated at 37°C with a heater.

Tissue preparation

Ten-week-old rats were anesthetized with urethane (1.5 g/kg, i.p.) and euthanized by exsanguination. The main branch of the superior mesenteric artery was isolated. After removal of fat and adventitia in normal physiological salt solution (PSS), the mesenteric artery was cut into rings (1 mm in diameter) for the measurement of isometric tension, histological analysis, and protein purification (17 – 19).

Immunohistochemical detection of MGO-derived AGEs (CEL and argpyrimidine)

The arterial preparations were fixed in 4% paraformaldehyde at 4°C overnight and incubated in the sucrose gradients (10% – 20%) at 4°C for 8 h. After they were embedded in OCT compound (Sakura Finetek, Tokyo), frozen sections (10-μm-thick) were made using a cryostat (Leica, Nussloch, Germany). Immunohistochemical staining for CEL and argpyrimidine was performed by a peroxidase staining kit (LSAB2; Dako, Glostrup, Denmark) according to the manufacturer's instructions. Mouse monoclonal antibodies against CEL (Trans Genic, Kobe) and argpyrimidine (Nichiyu, Tokyo) were used as the primary antibodies. Images were obtained with a light microscope (BX-51; Olympus, Tokyo) equipped with a CCD camera (MicroPublisher 5.0 RTV; Roper Industries, Sarasota, FL, USA). Image J software was used for the quantitative analysis.

Measurement of isometric tension

The arterial preparations were placed in normal PSS, which contained 136.9 mM NaCl, 5.4 mM KCl, 1.5 mM $CaCl_2$, 1.0 mM $MgCl_2$, 23.8 mM $NaHCO_3$, 5.5 mM glucose, and 0.001 mM EDTA. The high KCl solution was

prepared by replacing NaCl with equimolar KCl. These solutions were saturated with a 95% O_2 – 5% CO_2 mixture at 37°C and pH 7.4. Smooth muscle contractility was recorded isometrically with a force-displacement transducer (Nihon Kohden, Tokyo) as described previously (14 – 19). The arterial preparations were equilibrated for 30 min under a resting tension of 0.5 g. They were then repeatedly exposed to 72.7 mM KCl solution until the responses became stable (45 min). Concentration–responses curves were obtained by the cumulative application of Ang II (0.1 – 10 nM). Concentration–responses curves to ACh (0.1 nM – 3 μM) and SNP (0.01 – 300 nM) were obtained by the cumulative applications to the artery pre-contracted equally with submaximal concentrations of NA (300 nM – 3 μM). Effects of acute treatment (15 min) with a specific inhibitor of NOX, gp91ds-tat (1 μM), or a specific inhibitor of AT2R, PD123319 (10 μM), on ACh-induced relaxation or Ang II-induced contraction of SHR (10-week-old) mesenteric artery were also examined.

Fluorometric measurement of ROS

Levels of ROS production were measured by using a ROS-sensitive dye, 2′,7′-dichlorohydrofluroscin diacetate (H_2DCFDA) (Invitrogen, Carlsbad, CA, USA) (16). The frozen sections (10-μm-thick) were treated for 30 min with H_2DCFDA (100 nM). Images were obtained with a fluorescence microscope (BX-51). Image J software was used for the quantitative analysis.

Western blotting

Western blotting was performed as described previously (15, 17, 20, 21). Protein lysates were obtained by homogenizing the arterial preparations in Triton-based lysis buffer (1% Triton X-100, 20 mM Tris, pH 7.4, 150 mM NaCl, 1 mM β-glycerol phosphate, 1 mM NA_3VO_4, 1 μg/mL leupeptin, and 0.1% protease inhibitor mixture; Nacalai Tesque, Kyoto). Protein concentration in the lysate was measured using a bicinchoninic acid method (Pierce, Rockford, IL, USA). Equal amounts of proteins (8 – 15 μg) were separated by SDS-PAGE (7.5% – 15%) and transferred to a nitrocellulose membrane (Pall Corporation, Ann Arbor, MI, USA). After being blocked with 0.5% skim milk, membranes were incubated with primary antibodies (1:200 – 500 dilution) at 4°C overnight and then visualized using horseradish peroxidase–conjugated secondary antibodies (1:10,000 dilution, 1 h) and the EZ-ECL system (Biological Industries, Kibbutz Beit Haemek, Israel). Equal protein loading was confirmed by measuring total actin expression.

Statistical analysis

Results are expressed as the mean ± S.E.M. Statistical evaluation of the data was performed by Student's *t*-test between two groups and ANOVA followed by Bonferroni's test between three groups. Results were considered significant when the *P*-value was less than 0.05.

Results

Accumulation of MGO-derived AGEs in mesenteric artery from SHR

We firstly examined whether MGO accumulation increased in vascular walls of 10-week-old SHR by using immunohistochemical staining. In mesenteric artery from SHR, the accumulation of MGO-derived AGEs, CEL and argpyrimidine, significantly increased, and the AG treatment (1 g/L in water, 5 weeks) reversed it (Fig. 1: A, B, n = 6, $P < 0.05$ between SHR and WKY, $P < 0.05$ between SHR+AG and SHR).

The changes of BP over time (5 – 10-week-old rats)

We next examined whether MGO accumulation affects BP. The SBP, MBP, and DBP were significantly higher in SHR, and the AG treatment partially but significantly normalized them (Fig. 2: A – C, n = 8, $P < 0.01$ between SHR and WKY, $P < 0.05$, $P < 0.01$ between SHR+AG and SHR).

Effect of MGO accumulation on Ang II-induced contraction and ACh- or SNP-induced relaxation in mesenteric artery

We next examined whether MGO accumulation affects vascular reactivity. In mesenteric artery from SHR (10-week-old), Ang II (0.1 – 10 nM)-induced contraction significantly increased, and the AG treatment (1 g/L in water, 5 weeks) reversed it (Fig. 3A and Table 1, n = 8). We observed that KCl (5.4 – 72.7 mM)-induced contraction was similar in three conditions (n = 4, data not shown). In mesenteric artery from SHR (10-week-old), ACh (0.1 nM – 3 μM)-induced relaxation was significantly impaired as was previously reported (22), and the AG treatment significantly normalized it (Fig. 3B and Table 1, n = 16). On the other hand, SNP (0.01 – 300 nM)-induced endothelium-independent relaxation in SHR did not change compared with WKY (Fig. 3C and Table 1, n = 6) as was also previously reported (22).

Effect of MGO accumulation on ROS production in mesenteric artery

To explore mechanisms through which MGO accumulation alters vascular reactivity, ROS production was measured by H_2DCFDA staining. In the mesenteric artery from SHR (10-week-old), ROS production significantly increased, and the AG treatment (1 g/L in water, 5 weeks) significantly normalized it (Fig. 4A, n = 9, $P < 0.01$ be-

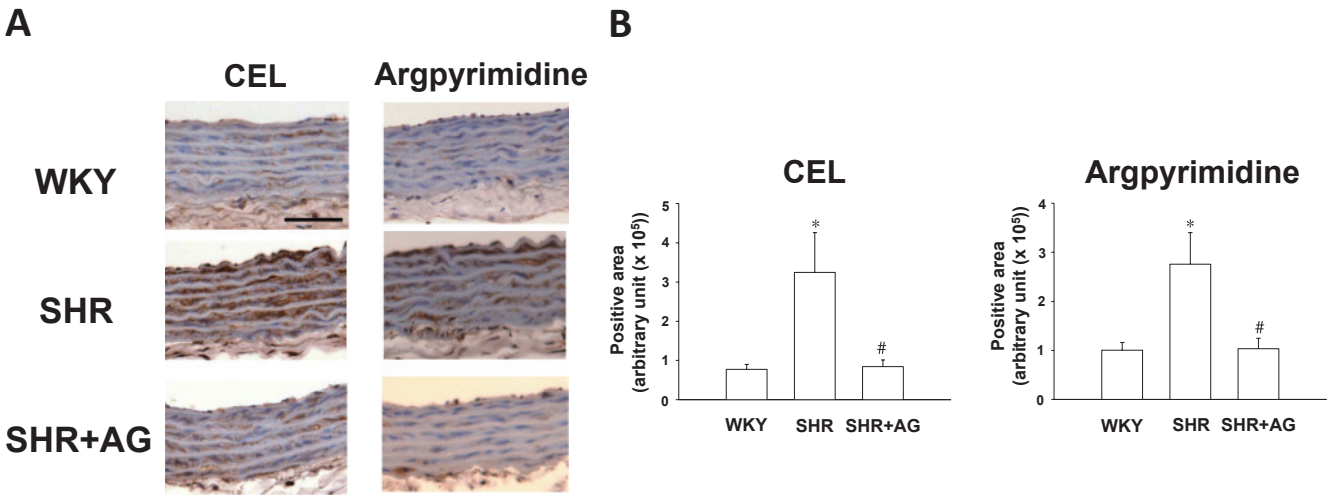

Fig. 1. Accumulation of methylglyoxal (MGO)-derived advanced glycation end-products (AGEs) in mesenteric artery from spontaneously hypertensive rats (SHR). A) Representative photomicrographs of immunohistochemically stained sections against antibodies to MGO-derived AGEs, N^{ε}-carboxyethyl-lysine (CEL) and argpyrimidine in isolated mesenteric artery (n = 6) from 10-week-old Wistar-Kyoto rats (WKY) or age-matched SHR treated without or with an MGO scavenger, aminoguanidine (AG) (1 g/L in water, for 5 weeks). Scale bar: 50 μm. B) Areas of positive staining were measured using Image J software and the results were shown as arbitrary units. $^{*}P < 0.05$ SHR vs. WKY, $^{\#}P < 0.05$ SHR+AG vs. SHR.

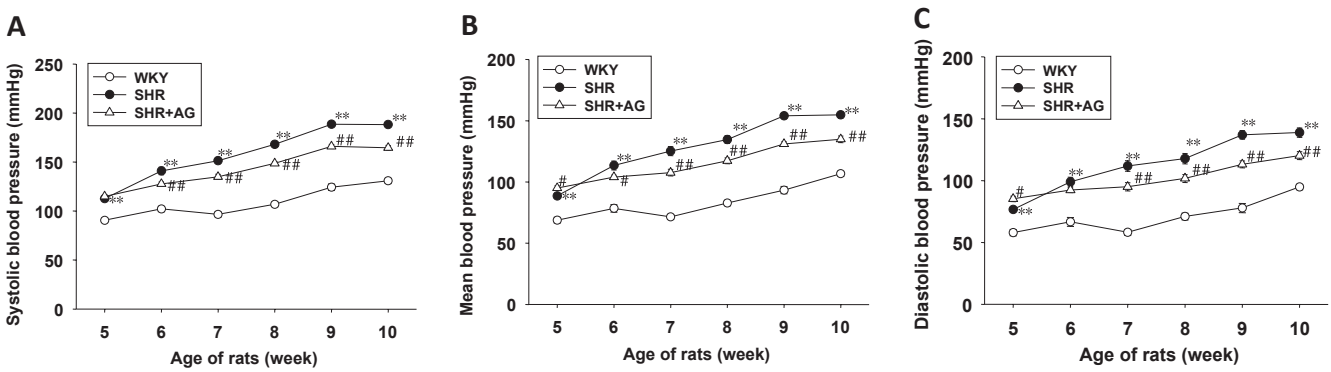

Fig. 2. The changes of blood pressure over time (5 – 10-week-old rats). Systolic blood pressure (A), mean blood pressure (B), and diastolic blood pressure (C) in the WKY (open circle) or SHR treated without (closed circle) or with AG (1 g/L in drinking water, open triangle) were measured by a tail-cuff method (n = 8) at a weekly interval. Results were expressed as the mean ± S.E.M. $^{**}P < 0.01$ SHR vs. WKY; $^{\#}P < 0.05$, $^{\#\#}P < 0.01$ SHR+AG vs. SHR.

tween SHR and WKY, $P < 0.05$ between SHR+AG and SHR). To further examine the involvement of ROS in the changes induced by MGO accumulation, we used a specific NOX inhibitor. Acute treatment (15 min) of mesenteric artery from SHR (10-week-old) with gp91ds-tat (1 μM) had no effects on the Ang II (0.1 – 10 nM)-induced contraction (Fig. 4B and Table 2, n = 4). In contrast, acute treatment of mesenteric artery from SHR with gp91ds-tat significantly enhanced the ACh (0.1 nM – 3 μM)-induced relaxation (Fig. 4C and Table 2, n = 5).

Effect of MGO accumulation on protein expression of NOX, eNOS, and SOD in mesenteric artery

In order to explore mechanisms of increased ROS by MGO accumulation, we next analyzed expression levels of NOX isoforms by western blotting. In mesenteric artery from SHR (10-week-old), NOX1 expression significantly increased, and the AG treatment (1 g/L in water, 5 weeks) reversed it (Fig. 5A, n = 7, $P < 0.01$ between SHR and WKY, $P < 0.01$ between SHR+AG and SHR). NOX2 expression significantly increased in SHR, but the AG treatment did not significantly normalize it (Fig. 5B,

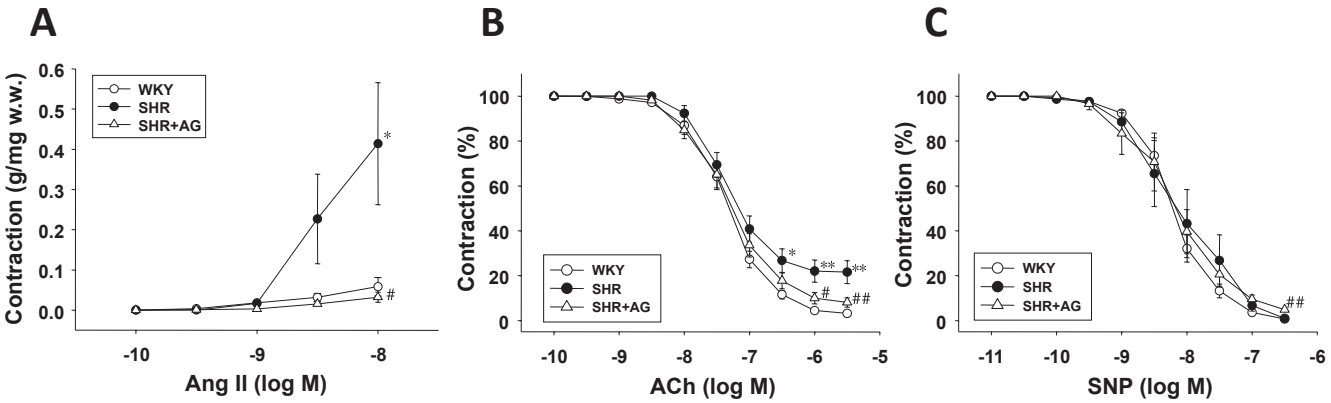

Fig. 3. Effect of MGO accumulation on vascular reactivity. A) Concentration–contraction relationships to angiotensin (Ang) II in mesenteric artery from 10-week-old WKY (open circle) or age-matched SHR treated without (closed circle) or with AG (1 g/L in water, for 5 weeks, open triangle). Ang II (0.1 – 10 nM) was cumulatively added. Contraction was expressed as an absolute value [g/mg wet weight (w.w.), n = 8]. B) Concentration–contraction relationships to acetylcholine (ACh) in mesenteric artery from 10-week-old WKY (open circle) or SHR treated without (closed circle) or with AG (open triangle). C) Concentration–contraction relationships to sodium nitroprusside (SNP) in endothelium-denuded mesenteric artery from 10-week-old WKY (open circle) or SHR treated without (closed circle) or with AG (open triangle). ACh (0.1 nM – 3 μM, n = 16) or SNP (0.01 – 300 nM, n = 6) was cumulatively added after the pre-contraction induced by noradrenaline (NA) (300 nM – 3 μM) had reached a steady state. NA-induced pre-contraction did not differ between the groups. 100% represents the NA-induced pre-contraction. Results were expressed as the mean ± S.E.M. *$P < 0.05$, **$P < 0.01$ SHR vs. WKY; $^{\#}P < 0.05$, $^{\#\#}P < 0.01$ SHR+AG vs. SHR.

Table 1. E_{max} and/or PD_2 for angiotensin (Ang) II-induced contraction, acetylcholine (ACh)-induced relaxation, and sodium nitroprusside (SNP)-induced relaxation

	WKY	SHR	SHR+AG
Ang II E_{max} (g/mg w.w.)	0.06 ± 0.00 (8)	0.41 ± 0.15* (8)	0.03 ± 0.01$^{\#}$ (8)
ACh E_{max} (%)	97.4 ± 0.7 (16)	79.6 ± 4.9** (16)	92.3 ± 2.1$^{\#\#}$ (16)
PD_2	7.3 ± 0.3	7.3 ± 0.3	7.3 ± 0.3
SNP E_{max} (%)	98.7 ± 0.7 (6)	99.0 ± 0.5 (6)	95.2 ± 0.9$^{\#\#}$ (6)
PD_2	8.2 ± 0.3	8.1 ± 0.2	8.3 ± 0.3

Mesenteric artery from 10-week-old Wistar-Kyoto rats (WKY) or age-matched spontaneously hypertensive rats (SHR) was treated without or with aminoguanidine (AG) (1 g/L in water, for 5 weeks). Results were expressed as the mean ± S.E.M. *$P < 0.05$, **$P < 0.01$: SHR vs. WKY, $^{\#}P < 0.05$, $^{\#\#}P < 0.01$: SHR+AG vs. SHR. The sample numbers are given in parentheses.

n = 10, $P < 0.05$ between SHR and WKY). The expression level of eNOS was similar between the groups (Fig. 5C, n = 8). We further examined whether MGO accumulation attenuated expression of anti-oxidant proteins. In mesenteric artery from SHR (10-week-old), expression of SOD-1 (Fig. 5D, n = 7) and SOD-2 (Fig. 5E, n = 7) did not change. The expression level of SOD-3 slightly increased in SHR, which was not statistically significantly level (Fig. 5F, n = 7).

Effect of AT2R blocker on the enhancement of Ang II-induced contraction in mesenteric artery

To explore mechanisms responsible for the enhancement of Ang II-induced contraction in SHR mesenteric artery, we used an AT2R blocker. Acute treatment (15 min) of mesenteric artery from SHR (10-week-old) with PD123319 (10 μM) significantly inhibited the Ang II (0.1 – 10 nM)-induced contraction (Fig. 6A and Table 2, n = 8). We also analyzed the expression level of AT2R. In mesenteric artery from SHR (10-week-old), AT2R expression significantly increased, and the AG treatment (1 g/L in water, 5 weeks) significantly normalized it (Fig. 6B, n = 7, $P < 0.01$ between SHR and WKY, $P < 0.05$ between SHR+AG and SHR).

Discussion

In the present study, we examined whether MGO accumulation in vascular walls affects BP and vascular reactivity in SHR. The major findings of the present

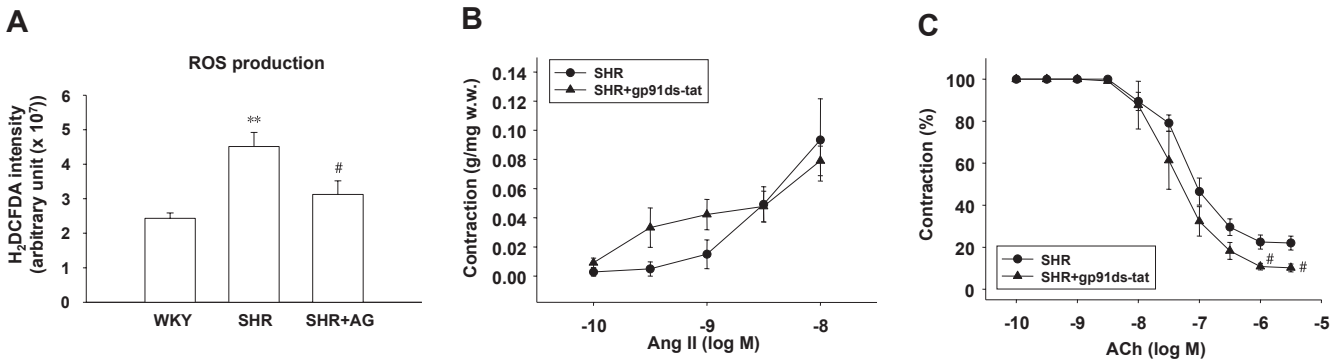

Fig. 4. Effect of MGO accumulation on reactive oxygen species (ROS) production in mesenteric artery. A) ROS production as determined by a 2′,7′-dichlorohydrofluroscin diacetate (H_2DCFDA) staining in mesenteric artery from 10-week-old WKY or SHR treated without or with AG (1 g/L in water, for 5 weeks). Fluorescent intensity of H_2DCFDA was measured using Image J software and the results are shown as arbitrary units (n = 9). B) Concentration–contraction relationships to Ang II in mesenteric artery from 10-week-old SHR acutely treated without (n = 4, closed circle) or with a specific inhibitor of nicotinamide adenine dinucleotide phosphate (NADPH) oxidase (NOX), gp91ds-tat (1 μM, for 15 min, n = 4, closed triangles). Ang II (0.1 – 10 nM) was cumulatively added. Contraction was expressed as an absolute value (g/mg w.w.). C) Concentration–contraction relationships to ACh in mesenteric artery from 10-week-old SHR acutely treated without (n = 8, closed circles) or with gp91ds-tat (1 μM, for 15 min, n = 5, closed triangles). ACh (0.1 nM – 3 μM) was cumulatively added after the pre-contraction induced by NA (300 nM – 3 μM) had reached a steady state. 100% represents the NA-induced pre-contraction. Results are expressed as the mean ± S.E.M. $^{**}P < 0.01$ SHR vs. WKY, $^{\#}P < 0.05$ SHR+AG vs. SHR or SHR+gp91ds-tat vs. SHR.

Table 2. E_{max} and/or PD_2 for Ang II-induced contraction and ACh-induced relaxation

	SHR	SHR+Inhibitor
		+gp91ds-tat
Ang II E_{max} (g/mg w.w.)	0.09 ± 0.03 (4)	0.08 ± 0.01 (4)
		+gp91ds-tat
ACh E_{max} (%)	78.6 ± 3.3 (8)	90.8 ± 1.8$^{\#}$ (5)
PD_2	7.2 ± 0.3	7.4 ± 0.3
		+PD123819
Ang II E_{max} (g/mg w.w.)	0.10 ± 0.02 (8)	0.03 ± 0.01$^{\#}$ (8)

Mesenteric artery from 10-week-old SHR was acutely (15 min) treated with gp91ds-tat (1 μM) or PD123319 (10 μM). Results were expressed as the mean ± S.E.M. $^{\#}P < 0.05$: SHR+inhibitor vs. SHR. The sample numbers are given in parentheses.

study are as follows (Fig. 7): 1) in mesenteric artery from SHR, MGO accumulation increased, which was reversed by an MGO scavenger, AG; 2) AG partially normalized the increased BP in SHR, suggesting that MGO accumulation could be at least in part associated with increased BP; 3) in mesenteric artery from SHR, MGO accumulation was associated with the increased Ang II-induced contraction and impaired ACh-induced relaxation; 4) The enhancement of Ang II-induced contraction in SHR mesenteric artery might be at least in part due to increased AT2R expression; 5) The impairment of ACh-induced relaxation in SHR mesenteric artery might be at least in part due to increased ROS production through the induction of NOX protein. These results collectively indicate that MGO accumulation in mesenteric artery may mediate development of hypertension in SHR at least in part via the AT2R-mediated increased Ang II-induced contraction and the increased ROS-mediated impairment of endothelium-dependent relaxation.

Our data showed that accumulation of MGO increased in mesenteric artery from 10-week-old SHR. It was reported that the expressions of GLUT5 (fructose transporter) and an MGO synthase, aldolase B, increased in SHR aorta, while the expression of other MGO synthases including SSAO or CYP 2E1 and plasma glucose level did not increase (23, 24). It was thus proposed that increased MGO accumulation was mediated via aldolase B through increased fructose transporting in vascular tissues of SHR.

In the present study, we used AG as an MGO scavenger. It was previously reported that AG normalized the impaired endothelium-dependent relaxation in aorta from streptozotocin-induced diabetes mellitus mice (25) and the increased endothelin-1-induced contraction in aorta from type 2 diabetic Otsuka Long-Evans Tokushima Fatty rats (26). The mechanism of these effects was suggested to be the inhibition of AGEs formations by reacting with α,β-dicarbonyl compounds including MGO. Especially, AG strongly reacts with MGO (27). On the other hand, it is known that AG is an inhibitor of inducible NOS (iNOS) (28). Thus, it is likely that the effects of AG in the present study are not only due to scavenging

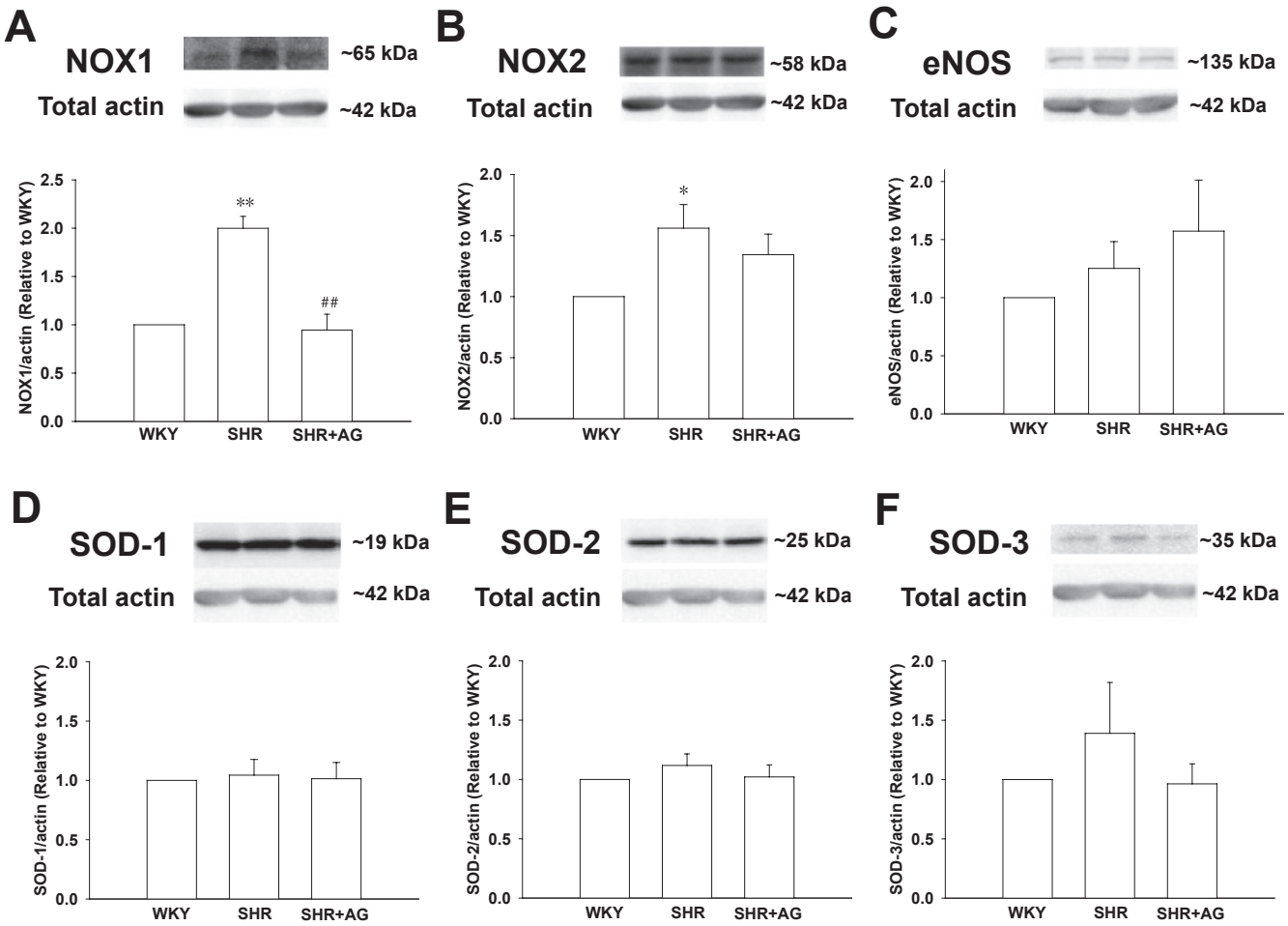

Fig. 5. Protein expression of NOX1 (n = 7, A), NOX2 (n = 10, B), endothelial nitric oxide synthase (eNOS) (n = 6, C), superoxide dismutase (SOD)-1 (n = 7, D), SOD-2 (n = 7, E), and SOD-3 (n = 7, F) in mesenteric artery from 10-week-old WKY or SHR treated without or with AG (1 g/L in water, for 5 weeks) as determined by western blotting. Equal protein loading was confirmed using total actin antibody. Relative protein expression to total actin was shown as fold increase relative to WKY. $^{*}P < 0.05$, $^{**}P < 0.01$ SHR vs. WKY; $^{\#\#}P < 0.01$ SHR+AG vs. SHR.

MGO but also due to the iNOS inhibition. However, since iNOS expression was not induced in SHR mesenteric artery (n = 3, data not shown) and AG potently reversed the MGO accumulation in SHR mesenteric artery (Fig. 1), it is suggested that the effects of AG are mostly likely due to the normalization of MGO accumulation.

Our data showed that MGO accumulation in mesenteric artery may mediate the increased Ang II-induced contraction in SHR. We previously demonstrated that short-term (30 min) MGO treatment augmented Ang II-induced contraction via enhancing NOX-derived ROS production in endothelium of rat carotid artery (16). In the present study, it was shown that MGO may mediate the increased ROS production in SHR mesenteric artery, which might be due to the induction of NOX1 protein. However, a specific NOX inhibitor failed to inhibit the Ang II-induced contraction in SHR mesenteric artery. It is generally known that Ang II interacts with both Ang II type 1 receptor, which mediates vasocontraction (29) and AT2R, which mediates vasorelaxation (30). However, there is a report demonstrating that AT2R also mediates smooth muscle contraction in mesenteric artery, especially from young SHR (5-week-old) (31). The present study showed that MGO accumulation may mediate the increased AT2R expression in mesenteric artery from SHR (10-week-old). Thus it is suggested that MGO accumulation may mediate the increased Ang II-induced contraction at least in part through the induction of contractile AT2R in relatively young SHR. We need to think about the possibility that MGO affects contractile response in vascular smooth muscle cells in a non-specific manner. While we cannot completely exclude the possi-

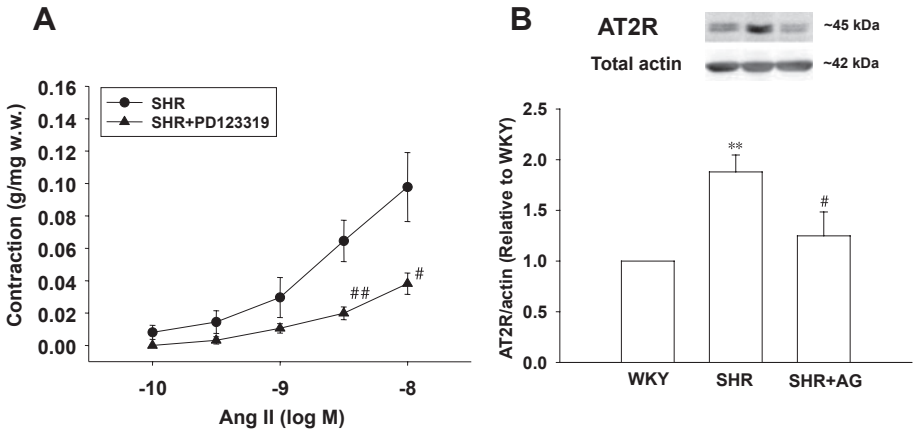

Fig. 6. Effect of Ang II type 2 receptor (AT2R) blocker on the enhancement of Ang II-induced contraction in mesenteric artery. A) Concentration–contraction relationships to Ang II in mesenteric artery from 10-week-old SHR acutely treated without (n = 8, closed circle) or with an AT2R blocker, PD123319 (10 μM, for 15 min, n = 8, closed triangles). Ang II (0.1 – 10 nM) was cumulatively added. Contraction was expressed as an absolute value (g/mg w.w.). Results are expressed as the mean ± S.E.M. B) Protein expression of AT2R in mesenteric artery from 10-week-old WKY or SHR treated without or with AG (1 g/L in water, for 5 weeks) was determined by western blotting. Equal protein loading was confirmed using total actin antibody. Relative protein expression to actin was shown as fold increase relative to WKY (n = 7). $^{**}P < 0.01$, SHR vs. WKY; $^{\#}P < 0.05$, $^{\#\#}P < 0.01$, SHR+PD vs. SHR or SHR+AG vs. SHR.

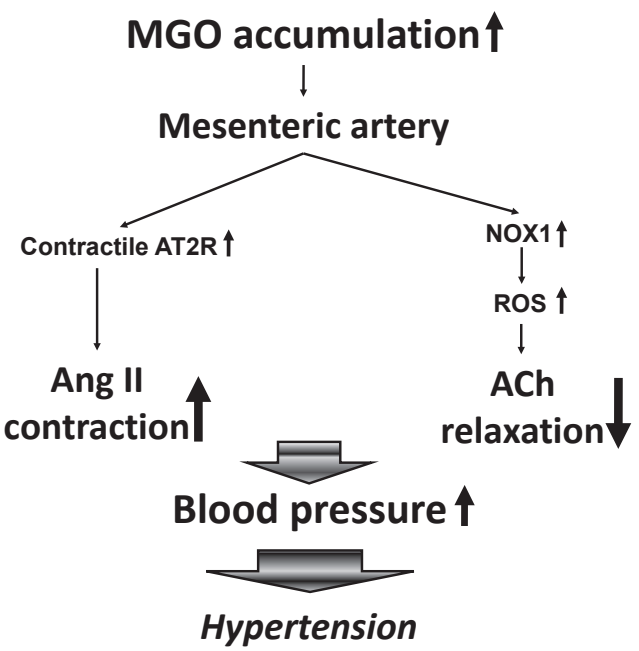

Fig. 7. Summary of the present results. MGO accumulation in mesenteric artery may mediate the development of hypertension in SHR at least in part via the AT2R-mediated increased Ang II-induced contraction and the increased ROS-mediated impairment of endothelium-dependent relaxation.

bility, it may not be applicable to the present result because it was observed that KCl-induced contraction was similar in three conditions (WKY, SHR, and SHR+AG). It should also be noted that some variations exist in the amplitude of the Ang II-induced contraction in SHR (10-week-old) mesenteric artery (Fig. 3A vs. Fig. 4B and Fig. 6A), indicating that this function (AT2R-mediated contraction) is dynamically changing in younger SHR.

Our data showed that MGO accumulation in mesenteric artery may mediate the impairment of ACh-induced endothelium-dependent relaxation in SHR. There is a study demonstrating that the increased MGO-derived AGEs may mediate the decrease of eNOS expression in aorta from SHR (14-week-old) (32). In the present study, however, eNOS expression did not decrease in mesenteric artery from SHR (10-week-old) compared with the age-matched WKY. There is a report demonstrating that eNOS expression did not decrease in mesenteric artery from SHR (31-week-old) (33), supporting the present results. On the other hand, the present study showed that protein expression of both NOX1 and NOX2 was augmented but AG specifically inhibited NOX1 induction in SHR mesenteric artery. We also provided evidence that a specific NOX inhibitor enhanced the ACh-induced relaxation in SHR mesenteric artery. Thus it is suggested that MGO accumulation may mediate the impairment of endothelium-dependent relaxation at least in part via NOX1-derived increased ROS, although we could not exclude the involvement of NOX2 and NOX4/5 which is also expressed in the vasculature (34). It is also proposed that NOX-derived ROS may cause both a decrease in NO bioavailability and a decrease in NO synthesis. Our data showed that AG treatment seems to completely inhibit

NOX1 expression (Fig. 5A), while it does not abolish ROS production (Fig. 4A). This discrepancy may be explained by the idea that NOX is not a solely source for ROS production in SHR mesenteric artery (e.g., xanthine oxidase and mitochondria).

Our data showed that MGO accumulation in mesenteric artery may mediate the increased protein expression of NOX1 and AT2R. The mechanisms of the increased expressions remain to be determined in the present study. We recently found that long-term (72 h) MGO treatment increased NOX1 expression via increasing activity and expression of NF-κB in rat isolated mesenteric artery (17). Thus it is presumed that MGO accumulation may mediate the increased expression of NOX1and AT2R in part through the activation of NF-κB signals in SHR mesenteric artery.

The present study explored the effects of MGO accumulation in vascular walls on contractile reactivity of isolated blood vessels. In mesenteric artery from SHR, MGO accumulation (in vivo) may mediate the increase of Ang II-induced contraction and the impairment of ACh-induced endothelium-dependent relaxation. We previously demonstrated in isolated carotid artery (in vitro) that short-term MGO treatment augmented the Ang II-induced contraction (16). It was also found that long-term (72 h) MGO treatment (in vitro) impaired the ACh-induced endothelium-dependent relaxation in rat isolated mesenteric artery (M. Mukohda and H. Yamawaki, unpublished observation). These in vitro results fit well to the present results in some aspects. On the other hand, there is a discrepancy between the result in an in vivo study and that in an in vitro study. It was observed that NA-induced contraction in SHR mesenteric artery seems to be enhanced compared with that in WKY mesenteric artery (n = 4, data not shown). We presumed that the enhanced NA-induced contraction may be at least in part due to the impairment of endothelium-dependent relaxing function. In contrast, we previously showed that in vitro MGO treatment (72 h) inhibited NA-induced contraction in endothelium-denuded mesenteric artery (17). Importantly, we demonstrated in the same report that the inhibitory effect of MGO was much more significant in endothelium-denuded than endothelium-intact mesenteric artery. It was thus presumed in endothelium-intact artery that the remaining endothelial-derived NO counteracts the MGO-induced ROS, which led to protection of smooth muscle from severely decreased contractility. Likewise, the present in vivo situation (endothelium-intact) and the previous in vitro situation (endothelium-denuded) are not the same, which may explain the discrepancy.

In conclusion, we demonstrated that MGO accumulation in mesenteric artery may mediate the development of hypertension in SHR at least in part via the AT2R-mediated increased Ang II-induced contraction and the increased NOX1-mediated impairment of endothelium-dependent relaxation. Further investigations on MGO may contribute to gain mechanistic insights into the roles of MGO on the pathogenesis of hypertensive vascular disease.

Acknowledgments

This study was supported in part by Grants for Scientific Research from the Kitasato University, School of Veterinary Medicine, and from the Japan Society for the Promotion of Science (JSPS).

References

1 Schalkwijk CG, van Bezu J, van der Schors RC, Uchida K, Stehouwer CD, van Hinsbergh VW. Heat-shock protein 27 is a major methylglyoxal-modified protein in endothelial cells. FEBS Lett. 2006;580:1565–1570.
2 Wu L. Is methylglyoxal a causative factor for hypertension development? Can J Physiol Pharmacol. 2006;84:129–139.
3 Desai KM, Chang T, Wang H, Banigesh A, Dhar A, Liu J, et al. Oxidative stress and aging: is methylglyoxal the hidden enemy? Can J Physiol Pharmacol. 2010;88:273–284.
4 Takatsume Y, Izawa S, Inoue Y. Modulation of Spc1 stress-activated protein kinase activity by methylglyoxal through inhibition of protein phosphatase in the fission yeast Schizosaccharomyces pombe. Biochem Biophys Res Commun. 2007;363:942–947.
5 Yim HS, Kang SO, Hah YC, Chock PB, Yim MB. Free radicals generated during the glycation reaction of amino acids by methylglyoxal. A model study of protein-cross-linked free radicals. J Biol Chem. 1995;270:28228–28233.
6 Ahmed MU, Brinkmann Frye E, Degenhardt TP, Thorpe SR, Baynes JW. N-epsilon-(carboxyethyl)lysine, a product of the chemical modification of proteins by methylglyoxal, increases with age in human lens proteins. Biochem J. 1997;324:565–570.
7 Oya T, Hattori N, Mizuno Y, Miyata S, Maeda S, Osawa T, et al. Methylglyoxal modification of protein. Chemical and immunochemical characterization of methylglyoxal-arginine adducts. J Biol Chem. 1999;274:18492–18502.
8 Ahmed N, Thornalley PJ. Chromatographic assay of glycation adducts in human serum albumin glycated in vitro by derivatization with 6-aminoquinolyl-N-hydroxysuccinimidyl-carbamate and intrinsic fluorescence. Biochem J. 2002;364:15–24.
9 Ogawa S, Nakayama K, Nakayama M, Mori T, Matsushima M, Okamura M, et al. Methylglyoxal is a predictor in type 2 diabetic patients of intima-media thickening and elevation of blood pressure. Hypertension. 2010;56:471–476.
10 Wang X, Desai K, Chang T, Wu L. Vascular methylglyoxal metabolism and the development of hypertension. J Hypertens. 2005;23:1565–1573.
11 Sankaralingam S, Xu H, Jiang Y, Sawamura T, Davidge ST. Evidence for increased methylglyoxal in the vasculature of women with preeclampsia: role in upregulation of LOX-1 and arginase. Hypertension. 2009;54:897–904.
12 Vasdev S, Ford CA, Longerich L, Parai S, Gadag V, Wadhawan S. Aldehyde induced hypertension in rats: prevention by N-acetyl cysteine. Artery. 1998;23:10–36.

13 Guo Q, Mori T, Jiang Y, Hu C, Osaki Y, Yoneki Y, et al. Methylglyoxal contributes to the development of insulin resistance and salt sensitivity in Sprague-Dawley rats. J Hypertens. 2009;27:1664–1671.
14 Mukohda M, Yamawaki H, Nomura H, Okada M, Hara Y. Methylglyoxal inhibits smooth muscle contraction in isolated blood vessels. J Pharmacol Sci. 2009;109:305–310.
15 Mukohda M, Yamawaki H, Okada M, Hara Y. Methylglyoxal enhances sodium nitroprusside-induced relaxation in rat aorta. J Pharmacol Sci. 2010;112:176–183.
16 Mukohda M, Yamawaki H, Okada M, Hara Y. Methylglyoxal augments angiotensin II-induced contraction in rat isolated carotid artery. J Pharmacol Sci. 2010;114:390–398.
17 Mukohda M, Morita T, Okada M, Hara Y, Yamawaki H. Long-term methylglyoxal treatment impairs smooth muscle contractility in organ-cultured rat mesenteric artery. Pharmacol Res. 2012;65:91–99.
18 Morita T, Okada M, Hara Y, Yamawaki H. Mechanisms underlying impairment of endothlium-dependent relaxation by fetal bovine serum in organ-cultured rat mesenteric artery. Eur J Pharmacol. 2011;668:401–406.
19 Morita T, Yamawaki H, Okada M, Hara Y. Contractile characteristics of rat mesenteric artery after organ culture. J Vet Med Sci. 2010;72:1621–1627.
20 Yamawaki H, Saito K, Okada M, Hara Y. Methylglyoxal mediates vascular inflammation via JNK and p38 in human endothelial cells. Am J Physiol Cell Physiol. 2008;295:C1510–C1517.
21 Yamawaki H, Hara Y. Glyoxal causes inflammatory injury in human vascular endothelial cells. Biochem Biophys Res Commun. 2008;369:1155–1159.
22 Virdis A, Colucci R, Versari D, Ghisu N, Fornai M, Antonioli L, et al. Atorvastatin prevents endothelial dysfunction in mesenteric arteries from spontaneously hypertensive rats: role of cyclooxygenase 2-derived contracting prostanoids. Hypertension. 2009;53:1008–1016.
23 Bouhelal R, Loubatieres-Mariani MM, Mir AK. Investigation of the mechanism(s) of 8-OH-DPAT-mediated inhibition of plasma insulin in spontaneously hypertensive rats. Br J Pharmacol. 1990;100:173–179.
24 Liu J, Wang R, Desai K, Wu L. Upregulation of aldolase B and overproduction of methylglyoxal in vascular tissues from rats with metabolic syndrome. Cardiovasc Res. 2011;92:494–503.
25 Prevost G, Bulckaen H, Gaxatte C, Boulanger E, Beraud G, Creusy C, et al. Structural modifications in the arterial wall during physiological aging and as a result of diabetes mellitus in a mouse model: are the changes comparable? Diabetes Metab. 2011;37:106–111.
26 Nemoto S, Taguchi K, Matsumoto T, Kamata K, Kobayashi T. Aminoguanidine normalizes ET-1-induced aortic contraction in type 2 diabetic Otsuka Long-Evans Tokushima Fatty (OLETF) rats by suppressing Jab1-mediated increase in ET(A)-receptor expression. Peptides. 2012;33:109–119.
27 Thornalley PJ, Yurek-George A, Argirov OK. Kinetics and mechanism of the reaction of aminoguanidine with the alpha-oxoaldehydes glyoxal, methylglyoxal, and 3-deoxyglucosone under physiological conditions. Biochem Pharmacol. 2000;60:55–65.
28 Misko TP, Moore WM, Kasten TP, Nickols GA, Corbett JA, Tilton RG, et al. Selective inhibition of the inducible nitric oxide synthase by aminoguanidine. Eur J Pharmacol. 1993;233:119–125.
29 Mugabe BE, Yaghini FA, Song CY, Buharalioglu CK, Waters CM, Malik KU. Angiotensin II-induced migration of vascular smooth muscle cells is mediated by p38 mitogen-activated protein kinase-activated c-Src through spleen tyrosine kinase and epidermal growth factor receptor transactivation. J Pharmacol Exp Ther. 2010;332:116–124.
30 Siragy HM, Carey RM. The subtype 2 (AT2) angiotensin receptor mediates renal production of nitric oxide in conscious rats. J Clin Invest. 1997;100:264–269.
31 Endemann D, Touyz RM, Li JS, Deng LY, Schiffrin EL. Altered angiotensin II-induced small artery contraction during the development of hypertension in spontaneously hypertensive rats. Am J Hypertens. 1999;12:716–723.
32 Wang X, Chang T, Jiang B, Desai K, Wu L. Attenuation of hypertension development by aminoguanidine in spontaneously hypertensive rats: role of methylglyoxal. Am J Hypertens. 2007;20:629–636.
33 Hernanz R, Martin A, Perez-Giron JV, Palacios R, Briones AM, Miguel M, et al. Pioglitazone treatment increases COX-2 derived PGI(2) production and reduces oxidative stress in hypertensive rats. Role on vascular function. Br J Pharmacol. 2012;166:1303–1319.
34 Lassegue B, Griendling KK. NADPH oxidases: functions and pathologies in the vasculature. Arterioscler Thromb Vasc Biol. 2010;30:653–661.